Well-width and aluminum-concentration dependence of the exciton binding energies in GaAs/$Al_xGa_{1-x}As$ quantum wells

Massimo Gurioli, Juan Martinez-Pastor,* and Marcello Colocci
European Laboratory for Non Linear Spectroscopy and Department of Physics, University of Florence, Largo Enrico Fermi 2, 50125 Firenze, Italy

Antonio Bosacchi and Secondo Franchi
Consiglio Nazionale delle Ricerche, Maspec Institute, 43100 Parma, Italy

Lucio Claudio Andreani
Institut Romand de Recherche Numérique en Physique des Matériaux (IRRMA), PHB-Ecublens, CH-1015 Lausanne, Switzerland
and Department of Physics, "A. Volta," Università di Pavia, via Bassi 6, I-27100 Pavia, Italy†
(Received 21 December 1992)

A photoluminescence-excitation (PLE) study of the exciton binding energy in GaAs/$Al_xGa_{1-x}As$ quantum-well (QW) structures is reported. A line-shape fit of the PLE spectra, based on a correct evaluation of the absorption probability in QW's, is proposed as a powerful tool in order to deduce accurately the exciton binding energies even in samples where the 2*s* peak is unresolved. The experimental results obtained are in good agreement with recent accurate theories. In particular, we find a strong dependence of the heavy-hole exciton binding energy E_1 on the aluminum concentration of the $Al_xGa_{1-x}As$ barrier, in agreement with the predicted importance of the dielectric mismatch and conduction-band nonparabolicity in enhancing E_1. Finally, evidence of exciton binding energies larger than the two-dimensional limit in GaAs is found even in relatively thick QW's (50 Å) with AlAs barriers.

I. INTRODUCTION

Excitons are two-particle bound states arising from the Coulomb interaction between electrons and holes. In a simplified picture, which already contains much of the physics involved, excitons in bulk semiconductors have a hydrogenic spectrum, scaled by the effective mass and the dielectric constant. The resulting effective Rydberg, which measures the electron-hole binding energy, is rather small in the case of III-V semiconductors; it turns out to be only 4 meV for bulk GaAs crystals. As a consequence, free excitons in GaAs are mainly observed in absorption spectra, where they give rise to discrete peaks below the band gap, while extrinsic features usually dominate the photoluminescence (PL) spectra.

The picture changes in quantum-well heterostructures. The carrier confinement produces an enhancement of the electron-hole Coulomb interaction and the excitonic effects dominate the optical properties of GaAs/$Al_xGa_{1-x}As$ quantum wells. In fact, exciton recombination gives usually the main contribution to the PL spectra up to room temperature and, contrary to the bulk case, even excited exciton states can be observed in optical experiments. These peculiar features have prompted much large interest in the exciton properties of semiconductor quantum wells, resulting in a large number of publications devoted to this subject.

Since the first theoretical approaches[1-5] based on a two-band approximation with isotropic and parabolic dispersion, the main properties of excitons in quantum wells (QW's) have been explained showing that the reduction of the electron-hole separation produces an increase of both the binding energy and the oscillator strength. For an infinite barrier height a monotonic increase of the binding energy was predicted[1,2] that would eventually reach, for vanishing small well widths, the two-dimensional (2D) limit, namely four times the bulk value (16 meV for GaAs). However, it was soon realized that the 2D limit can never be reached if one takes into account the finite depth of the well.[3,5] As the well width is reduced below a critical value, the carrier wave function penetrates into the barrier regions and excitons become more and more delocalized. The binding energy, after reaching a maximum value smaller than the 2D limit, therefore decreases and, for vanishing well widths, it approaches the value of the bulk barrier material.[3,5] More accurate theories for excitons in QW's have been proposed recently that take into account several additional effects, such as the valence-band mixing,[6-8] the Coulomb coupling with other subbands,[8-10] the nonparabolicity of the conduction band,[8-10] and the dielectric mismatch.[10-12] All these contributions produce an increase of the exciton binding energy which, in thin GaAs/AlAs quantum wells, is eventually predicted to become even larger than the two-dimensional GaAs limit.[10]

The main experimental techniques used so far for measuring the exciton binding energy consist in magneto-optical[13-16] and photoluminescence excitation,[1,17-20] (PLE) experiments. The use of a magnetic field parallel to the interfaces enhances the highly excited exciton states in the optical spectra. However, in order to deduce the binding energy at zero magnetic field, an

extrapolation procedure has to be used. In very high quality samples both the first and the second exciton levels, usually denoted as $1s$ and $2s$, can be resolved as clear peaks even at zero magnetic field;[17,18] the energy difference $\Delta E = E(1s) - E(2s)$ can then be compared directly with the theoretical predictions. Unfortunately, this occurs in only a few samples, usually thick wells with small aluminum content ($x = 0.3$), where the control of the growth quality can be very good. More often the $2s$ exciton state is a weak structure on the continuum onset or is even completely unresolved and different procedures have been reported[1,19,20] in order to determine the $2s$ energy position in between the onset and the top of the continuum absorption. In particular the $2s$ exciton state is usually unresolved in the case of thin and ultrathin QW's where the simple theories for the exciton binding energy are expected to be less accurate the thinner the well.

In this paper we report an experimental study of the exciton binding energy in a set of $GaAs/Al_xGa_{1-x}As$ quantum-well structures by means of PLE techniques. A line-shape fit, based on a simple absorption formula for the excitonic region of QW's, is proposed in order to have a better estimate of the exciton binding energies particularly in thin samples where the $2s$ peak is not clearly resolved. The experimental data are eventually well reproduced by the fits and the evaluated binding energies are in good agreement with a recent accurate theory.[10] We observe a strong dependence of the binding energies on the aluminum content in the barrier. This feature, unexpected in the early simple models, is mainly due to some subtle effects such as the conduction-band nonparabilicity and the dielectric mismatch. In particular, for a 50-Å GaAs/AlAs QW we find a binding energy of the order of 17 meV, therefore higher than the 2D limit for GaAs.

The paper is organized as follows. In Sec. II we discuss the line-shape model for the exciton absorption spectra in QW's (including both the discrete levels and the continuum) and its validity when applied to fitting the PLE spectra. Section III, after a brief illustration of the experimental procedures, is devoted to the discussion of the results. The concluding remarks are given in Sec. IV. Appendixes A and B report details of the calculations for deriving the line-shape model. In Appendix C an interpolation formula for calculating (in a large range of parameters) the heavy- and light-hole exciton binding energy is proposed that reproduces with great accuracy the prediction of the theory reported in Ref. 10.

II. LINE-SHAPE MODEL

In this section we discuss a line-shape model for the optical absorption in QW's. For a single quantum well (SQW) having a width much smaller than the photon wavelength, the absorption of light cannot be described in terms of an exponential decay of the light intensity, as usually done in the bulk case. Therefore we define an absorption probability (a pure number), in terms of the absorbed energy per unit time and area A and the incident energy per unit time and area I, as[21]

$$w(\hbar\omega) = \frac{A}{I} = \frac{2\pi^2 e^2 \hbar}{n m_0 c} \sum_i f_i \delta(\hbar\omega - \hbar\omega_2) , \quad (1)$$

where n is the refractive index, m_0 is the bare electron mass, $\hbar\omega_i$ is the energy of the ith exciton transition,

$$f_i = \frac{2|\boldsymbol{\varepsilon}\cdot\mathbf{M}_i|^2}{\hbar\omega_i m_0 S} \quad (2)$$

is its oscillator strength per unit surface, $\mathbf{M}_i$ is the momentum matrix element between the initial and the final state of the ith transition, S is the area of the sample, and $\boldsymbol{\varepsilon}$ is the photon polarization vector.

Below the continuum edge, defined by $\hbar\omega = E_g$, the exciton spectrum consists in a sum of discrete levels. For energies larger than the edge ($\hbar\omega > E_g$) the sum over the quantum number describing the relative motion gives the following expression for the absorption probability per unit energy:

$$w(\hbar\omega) = \frac{2\pi^2 e^2}{n m_0 c} \tilde{f}_c(\hbar\omega)\rho(\hbar\omega) . \quad (3)$$

Here $\rho(\hbar\omega)$ is the joint density of states which, for parabolic bands, is proportional to the Heaviside step function $\Theta(\hbar\omega - E_g)$. The oscillator strength $\tilde{f}_c$ of the unbound exciton states can then be rewritten as

$$\tilde{f}_c(\hbar\omega) = \frac{2|\boldsymbol{\varepsilon}\cdot\mathbf{P}_{c-v}|^2}{K\omega S m_0} K(\hbar\omega) = f_c K(\hbar\omega) , \quad (4)$$

where $\mathbf{P}_{c-v}$ is the interband momentum matrix element. The enhancement factor $K(\hbar\omega)$ is known as the Sommerfeld factor and takes into account the residual interaction between electrons and holes. For purely 2D excitons this factor has been calculated by Shinada and Sugano;[22] they find

$$K_{2D}(\hbar\omega) = \frac{2\Theta(\hbar\omega - E_g)}{1 + \exp\{-\pi[E_{2D}/(\hbar\omega - E_g)]^{1/2}\}} , \quad (5)$$

where E_{2D} is the 2D exciton binding energy. The Sommerfeld factor is therefore 2 at the subband edge and slowly decreases to 1 on the energy scale of E_{2D}.

The enhancement factor in QW's has been calculated by Chan[23] for the $GaAs/Al_{0.3}Ga_{0.7}As$ system using a two-band approximation. Due to the reduced electron-hole correlation compared to the 2D case, $K_{QW}(E_g)$ turns out to be in the range 1.3–1.4 for well widths varying between 200 and 50 Å. Then $K_{QW}(\hbar\omega)$ decreases to 1 on the energy scale of the exciton binding energy in QW's. Chan also demonstrated the continuity of the absorption probability at the subband edge. Using this property we have deduced, from the knowledge of the discrete spectrum of the excitons calculated with the theory of Ref. 10, the appropriate value of $K_{QW}(E_g)$ for the QW's investigated. For thin QW's (50 Å) we find excellent agreement with the results of Chan, while our estimate of $K_{QW}(E_g)$ turns out to be lower for thicker wells. We refer to Appendix A for a detailed discussion of this point.

In order to have an analytic expression for the Sommerfeld factor, we have scaled the Shinada-Sugano formula by the exciton binding energy E_1 in the QW's obtaining

$$K_{\mathrm{QW}}(\hbar\omega)=\frac{K_{\mathrm{QW}}(E_g)\Theta(\hbar\omega-E_g)}{1+\exp\{-\pi[E_1/(\hbar\omega-E_g)]^{1/2}\}} . \quad (6)$$

This expression can be assumed to be accurate only near the band edge (say in a range of E_1), i.e., in the region of interest within the purpose of this paper. On the other hand, several other effects such as coupling with other subbands or warping of the hole subbands will anyway modify the absorption for higher energies.

The absorption probability at the first heavy-hole exciton subband will then assume the form

$$w(\hbar\omega)=\frac{2\pi^2e^2\hbar}{nm_0c}\left[\sum_{i=1} f_i\delta(\hbar\omega-\hbar\omega_i)+f_cK_{\mathrm{QW}}(\hbar\omega)\rho(\hbar\omega)\right] , \quad (7)$$

where the sum now runs only over the discrete levels.

So far we have reviewed the absorption line shape in QW's. However, due to the small optical depth of a SQW, transmission measurements do not provide a useful experimental tool. Multiple quantum wells can indeed be used in order to enhance the optical efficiency, but the price to pay is an increase of the inhomogeneous effects. PLE spectra are usually employed as an alternative and very powerful technique in the case of QW's. They reflect the absorption spectra weighted by the relative efficiencies of the relaxation paths.[24] These last processes can obviously be not only sample dependent, but also they can depend on the chosen emission wavelength.

In the following we will assume that the relative efficiency of the relaxation path can be approximated by a single constant η_H for all the excited states of the heavy-hole exciton subband. Furthermore we will include in the fits the first light-hole exciton state, which in most cases lies quite near the heavy-hole continuum edge. The formula we propose for the exciton line shape of the PLE spectra is then

$$I(\hbar\omega)\propto f_1\delta(\hbar\omega-\hbar\omega_1)+\eta_Lf_L\delta(\hbar\omega-\hbar\omega_L)+\eta_H\sum_{i=2} f_i\delta(\hbar\omega-\hbar\omega_i)+\eta_Hf_cK_{\mathrm{QW}}(\hbar\omega)\rho(\hbar\omega) , \quad (8)$$

where η_L, f_L, and $\hbar\omega_L$ are the recombination efficiency, the oscillator strength, and the recombination energy of the first light-hole exciton, respectively.

Finally, in order to fit the experimental data, a phenomenological broadening must be taken into account. In the case of a Lorentzian line shape the convolution integral with the Sommerfeld factor can be performed analytically while a numerical integration has been performed for a Gaussian broadening. We refer to Appendix B for details.

III. EXPERIMENTAL PROCEDURE AND RESULTS

The samples on which measurements have been made are GaAs/$Al_xGa_{1-x}As$ SQW's grown by molecular-beam epitaxy (MBE) on undoped substrates at a temperature of the order of 600 °C. The well widths vary in the range 40–120 Å and three different aluminum contents have been chosen, $x=0.3$, 0.5, and 1.0. Each structure contains three or more wells of different width separated by thick barriers (200–300 Å) in order to decouple the carrier wave functions. The samples are nominally undoped.

Continuous-wave PL and PLE measurements have been performed at 4 K using a tunable Ar^+ pumped Ti:sapphire laser as excitation source. The PL signal was dispersed in a 60-cm double-grating monochromator and detected by standard photon-counting techniques.

In Fig. 1 we report the PLE spectra at a liquid-helium temperature of a 70-Å quantum well with barriers having an aluminum content of $x=0.5$. Different spectra in the figure refer to different points of the same sample. The first heavy- and light-hole exciton states are clearly resolved in the spectra, together with the onset of the continuum absorption. However, the relative intensities of different contributions depend, as shown in the figure, quite strongly on the position of the excitation spot on the sample. The most likely explanation for this observation, which justifies the phenomenological parameters η_i ($i=H,L$) in Eq. (8), is a different efficiency of the relaxation paths. The relevance of the relaxation process on exciton recombination has been the subject of recent investigations[25] and the relaxation efficiency is obviously reflected in the PLE line shape.[24] The dependence on the excitation spot position on the sample of the relative intensity of different structures in the PLE spectra is a clear evidence of the role that extrinsic effects play in determining the efficiency of the relaxation paths.

Typical experimental data and relative fits are reported in Fig. 2 for four different samples. The half width at half maximum (HWHM) of the exciton peaks are much smaller in the case of the thicker samples (we find 0.3 meV only for the 120-Å QW, which is of the order of the

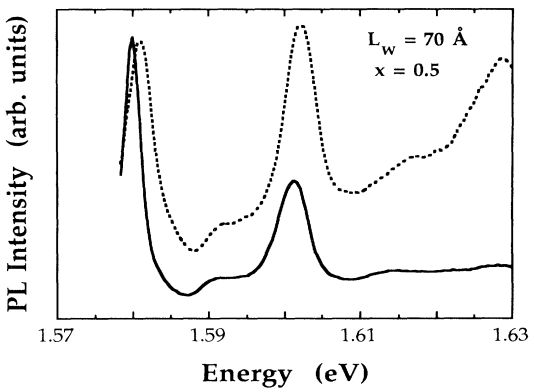

FIG. 1. PLE spectra at $T=4$ K of a 70-Å QW with an aluminum content in the barrier of $x=0.5$. Different lines refer to different positions of the excitation spot on the same sample.

homogeneous linewidth) while, decreasing the well width, the HWHM quickly becomes of the order of a few meV, denoting inhomogeneous effects. Nevertheless, the line shape of the PLE exciton peaks are not all Gaussian. In particular we find that the first heavy-hole exciton peaks are often asymmetric, showing a prominent high-energy tail. This extends up to the continuum absorption and therefore it must be taken into account when fitting this part of the spectrum. The physical origin of the tail is not at all clear; one possibility is the presence of unresolved replicas due to one monolayer fluctuations. Anyhow, since our interest is mainly devoted to extracting the binding energy of the heavy-hole exciton, we prefer to use a phenomenological approach, choosing the broadening shape in order to reproduce with the best accuracy the high-energy tail of the first heavy-hole exciton line. This allows us to reduce the number of free parameters that one would have in introducing a further Gaussian peak for the supposed exciton replica. In order to clarify this point we report in Fig. 2 the best fits obtained with both Gaussian (solid line) and Lorentzian broadening (dashed line); the Gaussian profile does not reproduce the region of interest, while a very nice fit is eventually obtained with a Lorentzian line shape.

In the case of the 40- and 80-Å wells having an aluminum content of $x=0.3$ [Figs. 2(a) and 2(b)] a weak structure, corresponding to the $2s$ state of the heavy-hole exciton, can be resolved on the rising edge of the absorption. The fits reproduce the line shape nicely and the energy spectrum of the heavy-hole exciton is in agreement with the theory presented in Ref. 10. Similar results are obtained for all the QW's with $x=0.3$.

On the other hand, the samples with a higher aluminum content that we have investigated do not show any resolved structure in correspondence of the $2s$ transition [see Figs. 2(c) and 2(d)]. As a matter of fact, the presence of the $2s$ peak and also the peak-to-valley ratio of the step is indeed sample dependent, most likely due, as reported in Ref. 20, to acceptor contamination during the MBE growth. In order to fit the PLE line shape we have used the heavy-hole exciton energy spectrum predicted by the theory keeping the energy of the first level E_1 as a free parameter. In practice we have first determined, by using the method reported in Appendix A, the parameter β from the theoretical sequence of the discrete exciton levels; then the exciton binding energy E_1 has been obtained from fitting the line shapes. The fit is indeed quite sensitive to E_1 since the ground-state binding energy determines the overall energy scale of the spectrum. The arrow in Fig. 2 indicates the position of the $2s$ state, as results from the fits. The position of the unresolved $2s$ level on the rising edge of the absorption has been discussed in the literature. In a early paper Miller *et al.*[1] took the $2s$ energy halfway up to the edge; in more recent works[17,20]

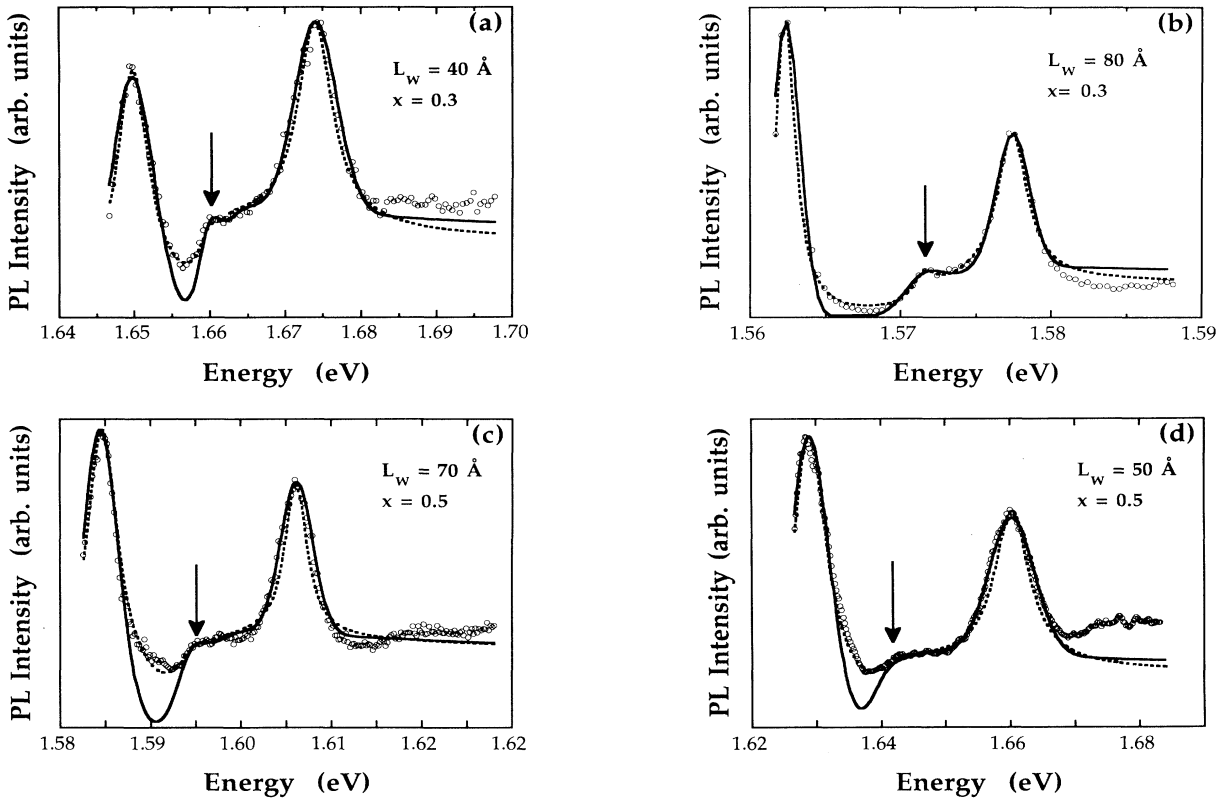

FIG. 2. PLE spectra at $T=4$ K of different QW's investigated: (a) $L_W=40$ Å, $x=0.3$; (b) $L_W=80$ Å, $x=0.3$; (c) $L_W=70$ Å, $x=0.5$; (d) $L_W=50$ Å, $x=0.5$. The circles are the experimental data; the solid (dashed) lines are fits with Gaussian (Lorentzian) broadening.

it has been chosen on the top of the step with the statement that the previous procedure would lead to underestimate the $1s$-$2s$ splitting. Our results seem to confirm the latter procedure; we believe, however, that only a line-shape fit can give an accurate estimate of the energy position of the excitonic levels.

The exciton binding energies obtained from the fits are reported in Fig. 3 as a function of the well width; different symbols refer to different aluminum content. The lines in the figure represent the theoretical predictions. For a general use the numerical results from the theory have been also fitted with an interpolation formula, reported in Appendix C, which allows us to obtain easily the exciton binding energies for a given well width and aluminum content. In fact, several papers[26–28] have been devoted very recently to the development of simple theories for calculating the exciton binding energies in QW's; here the aim was to reproduce with good accuracy the results of Ref. 10, avoiding, at the same time, complex calculations. The interpolation formula (C1) reaches this goal with a minimum effort.

The experimental data are found to be in agreement with the theory and also with other data reported in the literature.[13–18] However, the large majority of previous data refers to an aluminum content around $x=0.3$, which is known to give samples with the best optical quality. For higher aluminum content we find a remarkable increase of the exciton binding energy. As the theory predicts, this is not a consequence of an increase of the confinement since the exciton is already very well confined. It is rather a combined result of the conduction-band nonparabilicity and the dielectric constant mismatch. The conduction-band nonparabilicity yields an energy dependence of the electron effective mass which is further enhanced by the anisotropy of the conduction-band dispersion. The result is a strong dependence of the electron in-plane effective mass $m_{\parallel}^{*}$ on both the well width and the aluminum content of the barriers; for example, with $x=1$ and $L_W=50$ Å the effective mass becomes as large as $m_{\parallel}^{*}=0.1m_0$. The dielectric mismatch causes an effective image charge potential which modifies the Coulomb interaction between electrons and holes. It is an electrostatic effect yielding an increase of the exciton binding energies. Therefore the dependence of the exciton binding energy on the aluminum content of the barriers is a peculiar and important feature of the theory reported in Ref. 10, which turns out to be confirmed by our data. Similar results have been reported in Ref. 29, where, however, the physical origin of the increased exciton binding energy was not identified.

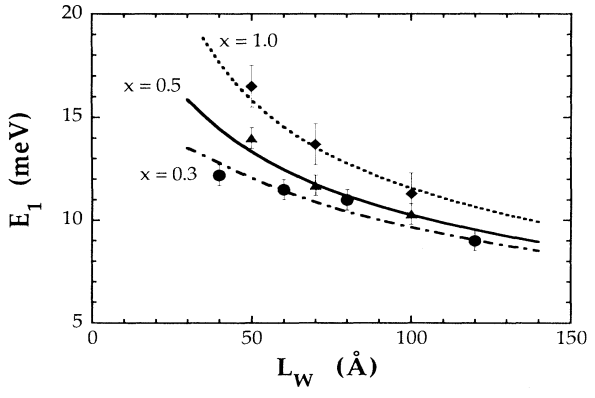

FIG. 3. Exciton binding energies of the QW's investigated. The lines refer to the theoretical predictions from the interpolation formula reported in Appendix C. Different symbols refer to different aluminum content: circles and dot-dashed line, $x=0.3$; triangles and solid line, $x=0.5$; diamonds and dotted line, $x=1.0$.

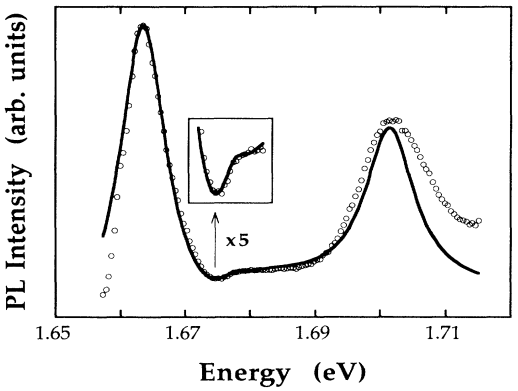

FIG. 4. PLE spectrum at $T=4$ K of a 50-Å QW with an aluminum content in the barrier of $x=10$. The solid line is the best fit with Lorentizian broadening. The inset shows an enlargement of the continuum absorption.

Of particular interest is the result for the 50-Å QW having an AlAs barrier where the exciton binding energy is found to be 17 meV. This value is indeed larger than the one corresponding to the GaAs 2D limit and that was predicted in the old exciton theories to be an unreachable upper limit. The PLE spectrum of this QW, together with the fit, is reported in Fig. 4. Unfortunately, the optical quality of this sample is not very good; the exciton lines are very asymmetric and a Lorentzian line shape, which nicely fits the high-energy tail of the heavy-hole exciton peak, cannot reproduce the low-energy wing of the light exciton band. At the same time the peak-to-valley ratio of the continuum absorption edge is only 1:10. Nevertheless, the model fits quite well, as shown in detail in the inset of Fig. 4, the continuum spectrum of the heavy-hole exciton demonstrating the usefulness of a model for the PLE line shape, particularly in the case of the unresolved $2s$ levels.

IV. CONCLUSION

A simple model for the PLE excitonic spectrum line shape in QW's taking into account also the continuum levels, has been suggested in order to deduce the excitonic binding energies even in the case of unresolved $2s$ peaks. Large values of the exciton binding energies have been found in the case of narrow wells cladded by $Al_xGa_{1-x}As$ barriers with a high aluminum content ($x=0.5, 1.0$) even larger than the GaAs 2D limit. Good

agreement has been found between the measured binding energies and the values predicted by the theory of Andreani and Pasquarello,[10] where the large binding energies result from subtle effects due to the conduction-band nonparabilicity, the dielectric mismatch, and the Coulomb interaction between different subbands.

ACKNOWLEDGMENTS

One of us (J.M.P.) acknowledges financial support from the Conselleria de Cultura, Educació i Ciencia de la Generalitat de Valècia and from the PFPI del Ministerio de Educatión y Ciencia. Work at IRRMAS was partially supported by the Swiss National Science Foundation under Grant No. 20-30272.90. Work at CNR-MASPEC is partially supported by CNR PF Materiali Speciali per Tecnologi Avanzate.

APPENDIX A

In this appendix we report an empirical method for evaluating the Sommerfeld enhancement at the continuum edge from the knowledge of the first few discrete levels of the exciton spectrum. The absorption continuity at the subband edge ($E=E_g$), obtained from Eq. (7), gives

$$\left[f_n \frac{dn}{dE} \right]_{E=E_g} = f_c K_{\mathrm{QW}}(E_g)\rho(E_g) \ . \tag{A1}$$

From this relation, knowing the analytic expressions of f_n and E_n (for instance, in the 2D case), one can extract the value of $K_{\mathrm{QW}}(E_g)$. Unfortunately, analytic expressions of E_n and f_n do not exist for excitons in QW's. We have then fitted the discrete energy spectrum of the QW's excitons calculated with the theory reported in Ref. 10 using the following expressions:

$$E_n = \frac{(1-\beta)^2 E_1}{(n-\beta)^2} \ , \quad f_n = \frac{(1-\beta)^3 f_1}{(n-\beta)^3} \ . \tag{A2}$$

Comparing Eq. (A2) with the ones reported in Ref. 27, the parameters β turns out to be related to the dimensionality α of the heterostructure, where $\alpha=3-2\beta$ is determined by the degree of anisotropy. In fact, for $\alpha=3$ (2) we obtain the hydrogeniclike spectrum in a isotropic 3D (2D) space. The numerical results are very well reproduced by this formula. For example, in the case of a 50-Å QW with $x=0.3$ we get from the exciton theory

$$E_1 = -12.08 \text{ meV} \ ,$$
$$E_2 = -1.96 \text{ meV} \ ,$$
$$E_3 = -0.76 \text{ meV} \ ,$$
$$f_1 = 79.81\times10^{-5} \text{ Å}^{-2} \ ,$$
$$f_2 = 5.26\times10^{-5} \text{ Å}^{-2} \ ,$$
$$f_3 = 1.27\times10^{-5} \text{ Å}^{-2} \ .$$

Equation (A2) with $\beta=0.327$ reproduces the previous results within the accuracy of the theory (of the order of 1%). Using the GaAs values [$f_c\rho(E_g)=1.57\times10^{-5}$ Å^{-2} meV^{-1} with the parameters reported in Ref. 21] we finally obtain $K_{\mathrm{QW}}(E_g)=1.42$, in excellent agreement with the value of 1.43 found by Chan. On the contrary, for wider wells we find values lower than Chan's results: in the case of a 190-Å QW we obtain $K_{\mathrm{QW}}(E_g)=1.1$ instead of 1.3. This discrepancy can be explained by taking into account that for a 190-Å well the heavy-light subband splitting is very small and the two-band model used by Chan is no longer valid. At the same time the calculation of the oscillator strength is very difficult in the case of thick wells and also the interpolation expressions are less accurate. The values of $K_{\mathrm{QW}}(E_g)$ and β obtained for the different QW's investigated are reported in Table I.

TABLE I. The values of β and $K_{\mathrm{QW}}(E_g)$, defined by Eqs. (A1) and (A2), respectively, are reported for the quantum wells investigated.

L_W (Å)	x	β	$K_{\mathrm{QW}}(E_g)$
40	0.3	0.336	1.47
60	0.3	0.319	1.38
80	0.3	0.294	1.31
120	0.3	0.260	1.20
50	0.5	0.330	1.48
70	0.5	0.304	1.38
100	0.5	0.264	1.28
50	1.0	0.302	1.58
70	1.0	0.269	1.44
100	1.0	0.223	1.31

APPENDIX B

We want to calculate the convolution integral between the continuum absorption and the chosen profile:

$$I_c = \int_{-\infty}^{+\infty} K_{\mathrm{QW}}(E')\rho(E')g(\hbar\omega-E',\Gamma_c)dE' \ , \tag{B1}$$

where Γ_c is the linewidth of the continuum transitions. In the case of a Lorentzian line shape I_c can be integrated directly following the method used by Goni *et al.*[30] in the case of bulk crystals. If we assume parabolic and isotropic band [$\rho(\hbar\omega)$ is proportional to the Heaviside step function $\Theta(\hbar\omega-E_g)$] and rewrite K_{QW} as

$$\frac{1}{1+\exp\{-2\pi/x\}} = \tfrac{1}{2}[1+\tanh(\pi/x)] \ , \tag{B2}$$

I_c splits in two parts,

$$I_c = [4K_{\mathrm{QW}}(E_g)\rho(E_g)\Gamma_c/\pi E_1](I_{c1}+I_{c2})$$

and we have

$$I_{c1} = \int_0^{\infty} \frac{x\,dx}{(x^2+\xi^2)^2+\gamma^2} = \frac{E_1}{\Gamma_c}\left[\pi - \frac{1}{2}\arctan\left[\frac{E_g-\hbar\omega}{\Gamma_c}\right]\right] \ , \tag{B3}$$

$$I_{c2} = \int_0^{\infty} \tanh\left[\frac{\pi}{x}\right] \frac{x\,dx}{(x^2+\xi^2)^2+\gamma^2} \ , \tag{B4}$$

where $x^2=4(E'-E_g)/E_1$, $\xi^2=4(E_g-\hbar\omega)/E_1$, and $\gamma=4\Gamma_c/E_1$. The integral I_{c2} can then be evaluated in

the complex plane by integration along the real axis and a upper hemicircle. The result is

$$I_{c2}=\pi\left[\frac{1}{4\gamma}\frac{2\sinh(\phi)}{\cosh(\phi)+\cos(\psi)}-\sum_m\frac{1}{\pi(m+\frac{1}{2})^3}\frac{1}{[\xi^2-1/(m+\frac{1}{2})^2]^2+\gamma^2}\right], \tag{B5}$$

where we have defined

$$\phi=\pi\frac{2a}{a^2+b^2}\ ,\quad \psi=\pi\frac{2b}{a^2+b^2}\ ,$$

$$a=\left[\frac{-\xi^2+\sqrt{\xi^4+\gamma^2}}{2}\right]^{1/2},$$

$$b=\left[\frac{\xi^2+\sqrt{\xi^4+\gamma^2}}{2}\right]^{1/2}.$$

APPENDIX C

In this appendix we report an interpolation formula for the binding energies of the ground-state heavy- and light-hole excitons in GaAs/$Al_xGa_{1-x}As$ QW's, valid in the following ranges of well widths L_W and aluminum content x:

$$30\ \text{Å}\le L_W\le 200\ \text{Å}\ ,\quad 0.25\le x\le 1.0\ .$$

Incorrect results are obtained when using this formula outside these ranges. The energies are calculated with the theory presented in Ref. 10. The fit is generally accurate within 0.1 meV, which is of the order, or even smaller, of the accuracy of the theory.

TABLE II. Values of the coefficients $A_{j,k}$ for energies in units of meV and well widths in units of 100 Å, entering the interpolation formula for the exciton binding energies given in Eq. (C1).

Exciton	j	$k=0$	$k=1$	$k=2$
heavy hole	1	27.909	3.325	−1.163
	2	−38.131	3.552	3.593
	3	30.417	−5.075	−5.232
	4	−10.389	6.289	0.789
light hole	1	31.401	−5.739	0.091
	2	−40.120	41.440	1.656
	3	27.250	−19.564	−29.228
	4	−8.960	3.894	19.393

The interpolation formula is

$$E(L_W,x)=\sum_{k=0}^{2}\sum_{j=1}^{4}A_{j,k}\frac{x^k}{(L_W+L_0)^j} \tag{C1}$$

with $L_0=50$ Å for both heavy- and light-hole excitons. In practice the calculated energies have been fitted with the sum of functions $1/(L_W+L_0)^j$ $(j=1,2,3,4)$; then a parabolic interpolation with respect to x has been performed. The coefficients $A_{j,k}$ are given in Table II for energies in unit of meV and widths in units of 100 Å. To give an example, for a well width of $L_W=100$ Å, L_W+L_0 must be set equal to 1.5 in formula (C1).

*On leave from Departament de Física Aplicada, Universitat de València, 46100 Burjassot, Valencia, Spain.
†Present address.

[1]R. C. Miller, D. A. Kleinmann, W. T. Tsang, and A. C. Gossard, Phys. Rev. B **24**, 1134 (1981).
[2]G. Bastard, E. E. Mendez, L. Chang, and L. Esaki, Phys. Rev. B **26**, 1974 (1982).
[3]R. L. Greene and K. K. Bajaj, Solid State Commun. **45**, 831 (1983).
[4]R. L. Greene, K. K. Bajaj, and D. E. Phelps, Phys. Rev. B **29**, 1807 (1984).
[5]M. Matsuura and Y. Shinozuka, J. Phys. Soc. Jpn. **53**, 3138 (1984).
[6]K. S. Chan, J. Phys. C **19**, L125 (1986).
[7]B. Zhu and K. Huang, Phys. Rev. B **36**, 8102 (1987); B. Zhu, *ibid.* **37**, 4689 (1988).
[8]L. C. Andreani and A. Pasquarello, Europhys. Lett. **6**, 259 (1988); Superlatt. Microstruct. **5**, 59 (1989).
[9]U. Ekenberg and M. Altarelli, Phys. Rev. B **35**, 7585 (1987).
[10]L. C. Andreani and A. Pasquarello, Phys. Rev. B **42**, 8928 (1990).
[11]D. M. Whittaker and R. J. Elliott, Solid State Commun. **68**, 1 (1988).
[12]M. Kumagai and T. Takagahara, Phys. Rev. B **40**, 12 359 (1989).
[13]D. C. Rogers, J. Singleton, R. J. Nicholas, C. T. Foxon, and K. Woodbridge, Phys. Rev. B **34**, 4002 (1986).
[14]A. S. Plaut, J. Singleton, R. J. Nicholas, R. T. Harley, S. R. Andrews, and C. T. Foxon, Phys. Rev. B **38**, 1323 (1988).
[15]M. Dutta, X. Liu, A. Petrou, D. D. Smith, M. Taysing-Lara, and L. Poli, Superlatt. Microstruct. **4**, 147 (1988).
[16]D. D. Smith, M. Dutta, X. C. Liu, A. F. Terzis, A. Petrou, M. W. Cole, and P. G. Newman, Phys. Rev. B **40**, 1407 (1989).
[17]P. Dawson, K. J. Moore, G. Duggan, H. I. Ralph, and C. T. B. Foxon, Phys. Rev. B **34**, 6007 (1986).
[18]D. C. Reynolds, K. K. Bajai, C. Leak, G. Peters, W. Theis, P. W. Yu, K. Alavi, C. Colvard, and I. Shidlovsky, Phys. Rev. B **37**, 3117 (1988).
[19]E. S. Koteles and J. Y. Chi, Phys. Rev. B **37**, 6332 (1988).
[20]D. F. Nelson, R. C. Miller, T. W. Tu, and S. K. Sputz, Phys. Rev. B **36**, 8063 (1987).
[21]L. C. Andreani, Ph.D. thesis, Scuola Normale Superiore, Pisa, 1989.
[22]M. Shinada and S. Sugano, J. Phys. Soc. Jpn. **21**, 1936 (1966).
[23]K. S. Chan, J. Phys. C **20**, 791 (1987).
[24]See, for instance, G. Bastard, in *Wave Mechanics Applied to Semiconductor Heterostructures* (Les Edition de Physique, Les Ulis Cedex, 1988), p. 275.
[25]Ph. Roussignol, C. Delalande, A. Vinattieri, L. Carraresi, and M. Colocci, Phys. Rev. B **45**, 6965 (1992).
[26]R. P. Leavitt and J. W. Little, Phys. Rev. B **43**, 2063 (1990).
[27]H. Mathieu, P. Lefebre, and P. Christol, J. Appl. Phys. **72**,

300 (1992); Phys. Rev. B **46**, 4092 (1992).
[28]R. Atanasov and F. Bassani, Solid State Commun. **84**, 71 (1992).
[29]S. Tarucha, H. Okamoto, Y. Iwasa, and N. Miura, Solid State Commun. **52**, 815 (1984).
[30]A. R. Goni, A. Cantarero, K. Syassen, and M. Cardona, Phys. Rev. B **41**, 10 111 (1990).